Activated carbon from biochar: Influence of its physicochemical properties on the sorption characteristics of phenanthrene

Junyeong Park [a], Ivan Hung [b], Zhehong Gan [b], Orlando J. Rojas [a,c], Kwang Hun Lim [d,*], Sunkyu Park [a,*]

[a] Department of Forest Biomaterials, North Carolina State University, Raleigh, NC 27695, United States
[b] National High Magnetic Field Laboratory, Tallahassee, FL 32310, United States
[c] School of Chemical Technology, Department of Forest Products Technology, Aalto University, FI-00076 Aalto, Espoo, Finland
[d] Department of Chemistry, East Carolina University, Greenville, NC 27858, United States

HIGHLIGHTS

- Elevated temperature and activation increased aromaticity and condensed carbons.
- Activation effects on mildly-treated biochars (<350 °C) were more substantial.
- Activated 350 °C-biochar removed phenanthrene fast and effectively.
- Activated 700 °C-biochar showed stronger binding with phenanthrene.
- Possibility for designing specialized biomass-based adsorbents was proposed.

ARTICLE INFO

ABSTRACT

The relationship between physicochemical properties of biochar-based activated carbons and its adsorption was investigated using an aromatic model compound, phenanthrene. Solid-state ^{13}C NMR analysis indicated more condensed aromatic structures when pyrolysis temperature increased or after activation process induced. The increasing aromaticity and non-protonated carbon fraction of the activated biochar treated at 300 °C amounted to 14.7% and 24.0%, respectively, compared to 7.4% and 4.4% for biochar treated at 700 °C. The surface area and pore volume were reduced with the increase in pyrolysis temperature, but increased after activation. Surface characteristics correlated with the initial sorption rate and equilibrium concentration of phenanthrene, but not with the aromaticity. Solid-state ^{2}H NMR for phenanthrene-d_{10} saturated activated biochars, however, showed substantial difference in molecular mobility, which might be due to the high aromaticity of the activated biochars. Overall, these results provide an opportunity to manipulate the characteristics of biomass-based adsorbents based on the application needs.

© 2013 Elsevier Ltd. All rights reserved.

1. Introduction

Thermochemical conversion of lignocellulosic biomass has been considered as a viable option to produce intermediate liquid streams for biofuels and biochemicals. During the conversion process, biochar is generated as a byproduct of pyrolysis; its optimization and application is essential to make the overall process economically feasible. Pyrolysis engineers have traditionally sought to minimize char production, as it has been considered as a low-value fraction, decreasing the yield of bio-oil. Recently, there is a growing interest in biochar due to the potential benefits of its application to soil as carbon sequestration and soil amendment (Chan et al., 2007; Novak et al., 2009; Woolf et al., 2010). It was also shown that biochar has promising sorption properties for various contaminants of water including polycyclic aromatic hydrocarbons (PAHs) and heavy metals (Chen and Chen, 2009; Kong et al., 2011; Sun et al., 2011; Uchimiya et al., 2011). Biochar made from renewable biomass has high surface area, ranging from 100 to 460 $m^2\,g^{-1}$ and present diverse surface sites such as carboxylic, phenolic, hydroxyl, and carbonyl groups (Novak et al., 2009). The physicochemical and porous properties of biochar are highly attractive for the development of effective and low-cost sorbents for removal of water contaminants.

Biochar can also be used as a precursor of value-added activated carbons. Recent studies have shown that steam activation of fast pyrolysis biochar greatly enhances the surface area and porous structure, and thus the sorption capacity for water contaminants (Lima et al., 2010). Chemical activation using KOH increased the surface area of biochar to values as large as 1500 $m^2\,g^{-1}$, comparable to those for commercial activated carbons (Azargohar and

Dalai, 2008). Optimization of the activation process may further improve porous structures and sorption capacity of activated biochar, which will help develop renewable alternatives to activated carbons made from coal. According to "Global Activated Carbon Market Forecast & Opportunities 2017", the demand for activated carbon is expected to increase more than 10% per year for the next 5 years to make it a $3 billion market by 2017 (Global Activated Carbon Market Forcast and Opportunities, 2012). The successful utilization of biomass to produce biofuels as well as activated carbon will not only help relieve environmental problems caused by coal mining, but also lower the production cost of effective sorbents that can be used in water treatment and wastewater reclamation.

In this study, it was hypothesized that the porous structure and sorption characteristics of activated biochar are dependent upon the physicochemical properties of the precursor biochar as well as the activation methods. In particular, aromatic structures in biochar may play an important role in the formation of porous networks during the activation process. The physicochemical properties of biochar are strongly dependent upon the nature of feedstock and pyrolysis conditions (e.g. heating temperature and residence time). Thus, an investigation of the biochar properties and sorption capacity of the activated counterparts is essential to identify optimum pyrolysis conditions.

In this study, conventional analytical methods as well as advanced solid-state NMR techniques were employed to determine the physicochemical properties of biochar prepared under different conditions. Solid-state NMR was used as a proven and effective tool for structural analyses of inhomogeneous solid samples. For example, ^{13}C solid-state NMR has provided quantitative structural information related to the aromaticity and the size of aromatic clusters (Brewer et al., 2009; Park et al., 2013). In addition, ^2H NMR was used to examine the dynamics of deuterated contaminants (phenanthrene) adsorbed on activated biochar, which provides valuable information as to the pore size. The porous properties of activated carbons such as surface area and pore volume have typically been examined through N_2 and CO_2 adsorption. The probe molecules are, however, much smaller than the actual water contaminants. Thus, ^2H NMR spectra from the actual sorbate allow detailed examination of pore size as well as binding affinity.

The present systematic investigation will help in the development of value-added materials from various sources of biomass and identify optimum processing conditions to produce biochars and to maximize the sorption capacity of activated carbons from the tailored biochars.

2. Methods

2.1. Sample production and activation

Debarked loblolly pine (*Pinus taeda*) chips were milled to pass through 20–40 mesh sieves and air-dried before further treatment. A porcelain boat containing 3 g of softwood mill was loaded into a quartz-tube furnace (MTI Corporation, Richmond, CA); the tube was purged for 10 min with nitrogen (1 L min^{-1} flow rate). During the purging, the boat with samples was placed outside the heating element of the furnace, then it was loaded into the preheated furnace and treated for 15 min with continuous nitrogen flow (1 L min^{-1}) at different temperatures (300, 350, 500, and 700 °C). Each treated sample was designated as "N-*treatment temperature*" (e.g. N-300 for the sample treated at 300 °C). After the heat treatment, the boat was removed from the furnace, and cooled down to ambient temperature under nitrogen flow. After weight loss measurement, all samples were stored in a desiccator before further treatment or analyses.

NaOH activation method was used to improve the sorption properties of biochar. Thermally-treated biochar (3 g) was mixed with 40 mL of 4 M NaOH aqueous solution and incubated at room temperature for 2 h under intermittent shaking (15 min intervals). After NaOH impregnation, the excess solution was discarded with vacuum filtering and the chemically-treated solid was dried overnight in an oven at 105 °C. The dried sample was heated in a quartz-tube furnace to 800 °C with a heating rate of 3 °C min^{-1} under inert atmospheric conditions (2 L min^{-1} N_2 flow) for 2 h. After activation, the samples were pulled out from the heating element and cooled down to ambient temperature under nitrogen flow. The activated samples were washed with 2 L of deionized (DI) water followed by 0.1 M HCl solution (200 mL) and washed again with DI water until the pH of filtrates was about 7.0. The washed activated carbon samples were dried in an oven set at 105 °C and stored in a desiccator for further analysis. Each activated sample was denoted as "N-*treatment temperature* AC" (e.g. N-300AC for activated carbon from N-300).

2.2. Characterization of biochar

Carbon, hydrogen, and nitrogen content in the thermally-treated and activated samples were analyzed by using a PerkinElmer 2400 Series II Elemental Analyzer (PerkinElmer, Waltham, MA). Oxygen content was calculated by subtraction of CHN and ash content from the total mass. Proximate analysis was conducted according to the ASTM standard D7582-10.

2.3. Solid-state ^{13}C NMR

Solid-state NMR spectra for the biochar samples were acquired with a Varian 3.2 mm MAS probe on a Varian Inova 500 spectrometer. For the DP/MAS (direct polarization/magic angle spinning) experiments, the sample was spun at a high frequency of 15 kHz. A dephasing time of 68 μs was used for dipolar dephasing experiments to determine non-protonated aromatic carbon fractions (Brewer et al., 2009, 2011). For the quantitative DP/MAS experiments, 1000–2000 FIDs were collected with a long acquisition delay of 60 s. The 90° pulse-lengths for ^1H and ^{13}C were 3.0 and 2.7 μs, respectively. The two-pulse phase-modulated (TPPM) decoupling scheme was employed with a radio-frequency field strength of 80 kHz. Quantitative spectral analysis was performed by integrating the assigned area of DP/MAS spectra and fractionating into three major categories – carbonyl, aromatic, and alkyl carbon fractions (Brewer et al., 2009). Quantification of the non-protonated aromatic carbon fraction was carried out in the same manner using DP/MAS and dipolar dephasing NMR spectra.

Long-range ^1H–^{13}C dipolar dephasing NMR experiments were also carried out to probe the size of the aromatic clusters. The QCPMG detection scheme (Larsen et al., 1998) was incorporated into the dephasing experiment for signal enhancement.

2.4. Static ^2H NMR

Solid-state ^2H NMR spectra for stationary samples were acquired using Varian Inova 500 spectrometer equipped with a Varian 3.2 mm MAS probe. A quadrupole echo pulse sequence with a refocusing delay of 30 μs was used. The 90° pulse-lengths for ^2H was 6.0 μs.

2.5. Surface characterization

BET (Brunauer–Emmett–Teller) surface area and pore-size distribution were measured by using N_2 adsorption. The adsorption of N_2 at 77 K was determined with a Micromeritics Gemini VII 2390p apparatus and the adsorption data was analyzed using

built-in calculation protocols. The BET surface area was calculated from the linear fit of the adsorption data. Micropore volumes were obtained by the *t*-plot method (Hu and Srinivasan, 1999), and the total pore volumes were estimated from the adsorbed amount of N_2 at a relative pressure of 0.99.

2.6. Adsorption test with a representative PAH – phenanthrene

To investigate adsorption property of the thermally-treated/activated samples with phenanthrene (Sigma–Aldrich, St. Louis, MO), a fixed amount of powdered biochar samples (sieved through 200 mesh screen) was mixed with a phenanthrene solution, then the concentration of phenanthrene was measured by UV–Vis spectrophotometer. 6.5 mg of phenanthrene was dissolved in 500 ml of methanol (HPLC grade), and DI water was added to make a total volume of 1 L solution. 30 mL of the prepared phenanthrene solution was mixed with 1 mg of the biochar sample and incubated at 25 °C for a fixed period of time. A commercial powdered activated carbon (NORIT® GAC 1240) was used in similar experiments as referent sorbent. After incubation, 1 mL of aliquot was centrifuged at 13,000 rpm for 5 min and the supernatant was analyzed by UV–Vis spectrophotometer at 251 nm wavelength to measure the concentration of phenanthrene. UV absorbance at 251 nm for phenanthrene solution with concentration between 0.05 and 6.5 mg L^{-1} was measured; the measured values showed a good linearity, R^2 = 0.999.

3. Results and discussion

3.1. Characterization of biochar before and after activation

Proximate analysis: The result of proximate analysis for the heat-treated samples showed substantial changes in volatile matter and fixed carbon (Table 1). With the increase in temperature, the content of volatile matter is substantially decreased from 87.4% in untreated feedstock to 10% in N-700, while the amount of fixed carbon is increased. The thermal breakdown and release of volatile matter are expected to be mainly from the carbohydrate fractions that are less stable during the heat treatment (Yang et al., 2007). Correspondingly, the content of fixed carbon increased with the increasing severity of the treatment conditions.

After the activation process, the mass fraction of volatile matter also decreased with the increased fixed carbon fractions. The changes in the mass fraction were more prominent in the N-300 and N-350 biochar samples. During the activation process, the volatile fraction in the biochar may be fused to more condensed aromatic structures and/or burned off, which may help to develop

porous structures. On the other hand, the changes in proximate analysis become less substantial for the N-500 and N-700. These results suggest that the biochar prepared under more severe pyrolysis conditions has more condensed structures resistant to thermal degradation during the activation process.

Ultimate analysis: Atomic O/C ratio from ultimate analysis data in Table 1 showed similar trends that those from proximate analyses. Large reductions in oxygen content and relatively higher carbon content were observed in the more severely treated biochar samples. This decrease in the oxygen content may arise from dehydration reactions, as well as the loss of volatile organic products and their release as gases (mostly of CO and CO_2). The decrease in O/C ratio after the activation process can also be explained by similar mechanisms. Previous studies reported that the relative content of acidic moieties on the surface decreases during activation processes (Chun et al., 2004; Li et al., 2009). The N-700 and N-700AC, however, showed a different trend in the atomic O/C ratio. This observation might be due to oxidation after the activation process, as reported that activated carbon treated at high temperature (1100 °C) for 1 h has relatively high oxygen content, presumably due to the re-oxidation by exposure to the atmosphere (Figueiredo et al., 1999).

3.2. Solid-state ^{13}C NMR

Biochar: Solid-state NMR spectroscopy was employed to obtain quantitative structural information of the thermally-treated lignocellulosic biomass. Previous studies have shown that heat treatment of biomass induces condensed aromatic structures in biochar. The changes in the aromatic structures were investigated with solid-state ^{13}C DP/MAS and recoupled ^1H–^{13}C dipolar dephasing NMR experiments, which was introduced to analyze woody biomass and biochars (Brewer et al., 2009; Czimczik et al., 2002). It was observed that the characteristic peaks of guaiacyl lignin in softwood, such as methoxyl groups (56 ppm) and C_3/C_4 (about 146–148 ppm) (Holtman et al., 2006), were substantially decreased with the increasing heating temperature. On the other hand, the NMR peak at around 130 ppm from the sp^2 carbons became more dominant at higher temperature in the ^{13}C DP/MAS spectra, suggesting that aromatic condensation took place after the heat treatment of woody biomass.

The combined DP/MAS and dephasing spectra were analyzed to obtain more quantitative structural information such as aromaticity (% fraction of total aromatic carbons in Table 2) (Brewer et al., 2009, 2011). The quantitative analysis of biochar samples indicated that with the increase in temperature, the amount of non-protonated aromatic carbons substantially increased, while the relative

Table 1
Proximate, atomic O/C ratio, and surface characteristics for the thermally-treated samples and their activated counterparts.

	Proximate analysis[a] (%)			Atomic O/C ratio[b]	BET surface area (m^2/g)	Pore volume (cm^3/g)	
	Volatile matter	Fixed carbon	Ash			Micropore[c]	Meso- and macropore[d]
Raw	87.4	11.0	1.55	0.632	0.38	n.d.[e]	n.d.
N-300	72.0	23.6	4.44	0.232	1.41	0.000	0.009
N-350	42.3	56.3	1.38	0.208	7.37	0.000	0.028
N-500	18.4	79.4	2.16	0.107	239	0.076	0.075
N-700	10.1	87.1	2.77	0.065	321	0.129	0.045
N-300AC	15.6	79.7	4.71	0.220	1250	0.289	0.783
N-350AC	20.7	77.4	1.87	0.165	702	0.241	0.246
N-500AC	12.5	86.5	1.01	0.093	346	0.128	0.162
N-700AC	14.5	83.8	1.73	0.107	57.0	0.013	0.041

[a] Dry-basis.
[b] Calculated based on ultimate analysis.
[c] *t*-plot micropore volume.
[d] Calculated by subtracting *t*-plot micropore volume from total pore volume.
[e] Not determined.

Table 2
Quantitative spectral analysis for solid-state ^{13}C DP/MAS NMR of the thermally-treated samples and their activated counterparts. The values were calculated based on 100% carbon in each biomass.

	Carbonyls (%)	Aromatics (%)				Alkyls (%)	Min. # of C in a cluster[a]
		C–O	Protonated	Non-protonated	Total aromatic		
Raw	4.1	4.7	a[b]	b[b]	44.1	51.8	–
N-300	3.4	8.1	18.1	26.9	53.2	43.4	–
N-350	3.7	10.4	14.9	38.9	64.2	32.1	–
N-500	3.6	6.0	20.0	46.4	72.5	24.0	11
N-700	5.1	7.3	4.9	56.7	68.9	26.1	16
N-300AC	12.3	12.6	4.4	50.9	67.9	19.78	12
N-350AC	4.8	8.2	4.2	59.7	72.2	23.1	20
N-500AC	6.9	11.6	1.2	63.8	76.5	16.7	27
N-700AC	7.2	12.5	2.8	61.1	76.3	16.5	23

[a] Estimated minimal number of carbons in an aromatic carbon cluster.
[b] Non-protonated carbon fraction for raw sample was not determined due to the low signal intensity of NMR spectrum with dipolar dephasing. The total amount of protonated and non-protonated aromatic carbon is 39.4% (a + b).

content of alkyl carbons significantly decreased. Total aromatic carbon fraction also increased, but after 500 °C, it slightly decreased (Table 2). The increases in the non-protonated aromatic carbon fraction suggest that the heat treatment induces a high degree of aromatic condensation, which may result in aromatic clusters of large sizes.

The size of the aromatic cluster was calculated from the quantitative NMR data in Table 2. Briefly, the number of carbons on the edge of aromatic cluster was estimated with the assumption that most dominant carbon species on the cluster edge are from the aromatic C–H and C–O. The estimated edge fraction, combined with the geometry of condensation, allowed us to calculate the minimum number of carbons in a cluster (detailed description can be found elsewhere (Brewer et al., 2009; Solum et al., 1989)). For the biochar produced under low pyrolysis temperatures <350 °C, it was impractical to estimate the cluster size due to the low degree of condensation and relatively large fraction of the alkyl carbons. The formation of aromatic clusters was observed at higher pyrolysis temperatures >500 °C (N-500 and N-700) and the size of the cluster was notably increased from N-500 to N-700 biochar samples.

The aromatic condensation (size of the aromatic cluster) was probed by long-range dipolar-recoupled dephasing experiments (Mao and Schmidt-Rohr, 2003). In the dephasing experiment, the NMR signal decreases during the dephasing time due to ^1H–^{13}C dipolar interactions (Fig. 1). The slower decay for the sample treated at a higher temperature indicates weaker dipolar interactions, and thus a larger average distance between the two nuclei. The relative content of the non-protonated carbons inside the cluster

would increase in a larger cluster, leading to the slower signal decay because of the weaker dipolar interactions. Thus, the slower signal change at higher temperature clearly suggests that the size of the aromatic cluster increased during the heat treatment, leading to a higher degree of aromatic condensation, as predicted from the non-protonated carbon fractions and the number of carbons in the cluster (Table 2).

Activated biochar: After the activation process, the NMR signals from the aliphatic carbons further were decreased, particularly for the N-300AC and N-350AC samples. The broader peak observed in activated samples at around 130 ppm indicates that more complex aromatic structures might be developed during the activation process. The quantitative analyses of the NMR spectra showed that the chemical activation using NaOH increased aromatic carbon fractions as well as the non-protonated carbon content (i.e. size of the cluster), indicating that more condensed aromatic structures were developed during the activation. These changes in carbon structure were more substantial when the woody biomass was treated at lower temperature prior to the activation process. These results suggest that the post-heat treatment of biochars induces the development of more condensed aromatic carbon structures by burning off the volatile carbon fraction and thermal transformation of structures, making solid products with higher aromaticity than their precursor biochars.

As for N-500AC, the number of carbons in a cluster was increased more than 2-fold, from 11 to 27. This substantial increase imply that despite the high aromaticity (72.5%), the carbon structure inside N-500 is amenable to further structural alteration, resulting in larger size of aromatic clusters. This larger cluster might be from condensation of non-aromatic carbon structures in N-500 or fusion of existing clusters. Compared to N-500AC, N-700AC showed a relatively lower increase in the number of carbons inside clusters, from 16 to 23. This might be due to that the N-700 has a more rigid structure and consequently less flexibility toward further structural changes, even with severe chemical and thermal treatment, like NaOH-activation.

3.3. Surface area and pore volume

Biochar: The surface area and pore volume of the biochars were measured before and after activation (Table 1). For the biochar samples, the BET analysis of N-300 and N-350 yielded very low values, less than 10 m^2 g^{-1}. Biochars prepared at higher temperatures (N-500 and N-700) exhibited higher BET surface areas, 239 and 321 m^2 g^{-1}, respectively, which are about one-third of those typical of commercial activated carbons.

Activated biochar: It has been shown that physical or chemical activation increases the surface area and pore volume of
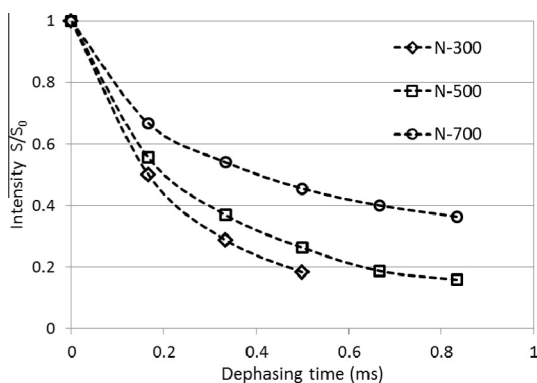

Fig. 1. Quantitative ^{13}C NMR analysis with long-range dipolar-recoupled dephasing experiments. Total aromatic carbon fraction includes non-protonated aromatic carbon and protonated aromatic carbon fractions.

carbonaceous materials (Chen and Chen, 2009; Chun et al., 2004). In fact, the surface area and pore volume greatly increased after the activation (Table 1). In particular, the activated counterpart from biochar prepared at a low pyrolysis temperatures (N-300AC) exhibited a surface and pore volume higher than those of the reference, commercial activated carbons (NORIT). It is also notable that activated counterparts from the biochar produced at a higher pyrolysis temperature have lower surface area and pore volume. As for N-700AC, there is a substantial decrease in surface area after the activation process, from 321 to 57 $m^2 g^{-1}$. This might be due to the thermal condensation of carbon structures inside the biochar. Our structural analyses showed that the low temperature pyrolysis biochar has a lower aromaticity and smaller aromatic cluster (Table 2 and Fig. 1). It was also shown that the N-300 biochar contains higher amount of alkyl carbons and volatile matter. The volatile carbon fraction almost completely disappeared after the activation process, implying the formation of highly porous structures by the thermal degradation of volatile carbons. Condensed aromatic structures might be more resistant to thermal degradation, and thus the pre-formed aromatic structures in biochar produced at a high pyrolysis temperature (>500 °C) may inhibit development of surface area and porous structures during the activation process.

3.4. Adsorption of phenanthrene on thermally-treated biomass

Biochar: The sorption ability of the biochar was tested for hydrophobic PAH (phenanthrene) (Fig. 2). It was expected for the biochar with a higher aromaticity to be better sorbent for aromatic compounds such as the PAHs, due to more favorable hydrophobic and π–π interactions (Boving and Zhang, 2004; Moreno-Castilla, 2004). In our study, biochar produced at higher temperatures had a higher aromaticity as well as larger surface area. However, the sorption capacity of N-700 for phenanthrene was very close to that of N-300 with much lower aromaticity and smaller surface area. These sorption results suggest that the BET surface area alone might not govern the adsorption of phenanthrene. Aliphatic regions of the biochar, as well as other structural or chemical properties of adsorbents may also contribute to the binding of the hydrophobic contaminant.

The adsorption kinetics of the biochar displayed similar trends. After the relatively efficient initial adsorption, the adsorption process was significantly slowed down over the longer incubation times. These results suggest that the binding sites of the biochar are not readily available to the adsorbents, which requires a long time to be saturated.
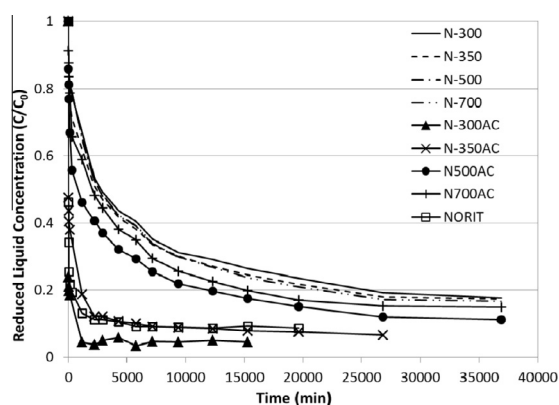

Fig. 2. Adsorption of phenanthrene onto thermally-treated biomass samples – removal of phenanthrene after different incubation time.

Activated biochar: The chemical activation of the biochar greatly enhanced sorption ability of the PAH (Fig. 2), particularly for the biochars prepared at lower pyrolysis temperatures (300 and 350 °C). It is also noted that N-300AC almost immediately adsorbs the hydrophobic contaminant, in a very short period of time (<3 min), which is ideal for water remediation. The activated biochar (N-300AC) also exhibited a good initial sorption efficiency (156 mg g^{-1}) after 30 min, which compares favorably against values for commercially available activated char prepared from coal (NORIT, 129.8 mg g^{-1}). However, when the lignocellulosic biomass was treated at a higher pyrolysis temperature followed by activation, no substantial changes in adsorption performance were observed.

To compare the adsorption kinetics of the generated samples, a pseudo-second order adsorption model was applied to the phenanthrene measured adsorption data (Fig. 2). This model can be expressed as below:

$$t/q = 1/(k_2 \cdot q_e^2) - (t/q_e)$$

where k_2 is the equilibrium rate constant of pseudo-second order sorption (g mg^{-1} min^{-1}) and q_e is the amount of adsorbed sorbate at equilibrium (mg g^{-1}) (Ho and McKay, 1998). The linear plot of t/q vs. t was fitted with the measured data to obtain the model parameters. N-500AC showed about 11% increase in q_e for phenanthrene removal, compared to the N-500 sample, and N-700AC showed less than 6% of difference with the N-700 sample. To find any correlation between the properties of adsorbents and the adsorption kinetics, several plots were tested along with linear regressions. Based on these observations, the total aromaticity of the thermally-treated samples is not well-correlated to the adsorption kinetics for phenanthrene, in both non-activated and activated samples ($R^2 < 0.06$). In contrast, BET surface area and total pore volume showed relatively good correlations with the amount of adsorption at equilibrium ($R^2 = 0.89$ and 0.86, respectively) and the initial adsorption rate ($R^2 = 0.61$ and 0.81, respectively).

The sorption kinetics of the activated biochar seems to be governed largely by other structural characteristics of the surface, such as BET surface area and pore volume. Furthermore, it may also be affected by the size of adsorbents. N-300AC was shown to have larger surface and pore volume, particularly pores larger than micropores, compared to other activated carbons (Table 1). The larger surface area may originate from the larger pores with diameters greater than 2 nm. The activated carbon with larger pores would be more efficient for removal of larger size contaminant, especially during the initial adsorption stage. If the size of target sorbate is large enough to slow down the access to micropores with diameters of less than 2 nm, then it will affect negatively the overall adsorption performance, as well as the correlation to the surface area and total pore volume. The larger pores may play an important role in the sorption for the large contaminant molecule. Valderrama and coworkers reported that the removal of organic molecules by activated carbon largely depends on the size of the organic compounds. It was shown that a large micropore (high surface area) is more efficient for the removal of small molecules, but for larger molecules such as PAHs, mesopores and macropores play more important roles in the adsorption (Valderrama et al., 2008).

Activated biochars prepared in this study are shown to have large surface area and pore volumes comparable to the commercial activated carbons. In particular, N-300AC has a large surface area and a much bigger fraction of pore volume from larger pores (Table 1). Although our NMR analyses showed that the activated carbon containing more mesopores has lower aromaticity, it exhibited better sorption capacity for the hydrophobic phenanthrene (3.6×7.0 Å). These results suggest that the larger pores consisting of smaller aromatic clusters in N-300AC may be more effective for

the phenanthrene adsorption than micropores with bigger clusters in the other activated biochars.

Combined with the effective removal of phenanthrene by adsorption using activated biochars, there could be more possibilities that can extend the application of these adsorbents for bioremediation. Since the physical and chemical adsorption cannot degrade pollutants into non-toxic substrates, bioremediation has been considered as a complementary process to remove pollutants by physical and chemical remediation (Peng et al., 2008; Sarkar et al., 2012). It has been reported that the activated carbon could be used as a microbial carrier to adsorb and degrade pollutants in a single system (Voice et al., 1992) and a recent study demonstrated the effective removal of phenanthrene using an adsorbent from a natural clay mineral, e.g. bentonite (Huang et al., 2013). Combination of sorption and biodegradation of pollutants using activated biochar, therefore, can be an interesting and promising application for bioremediation.

3.5. Solid-state ^{2}H NMR for phenanthrene-d$_{10}$-saturated samples

The surface area and pore volume of activated carbons have been typically measured by adsorption of N$_2$ and CO$_2$. The probe molecules are, however, much smaller than the actual contaminants and have different physical properties than the contaminants containing aromatic side chains. Thus, the surface area measured from the small molecule adsorption may not represent real binding sites for large contaminants with different physical properties.

Deuterium (^{2}H) is a spin $I = 1$ nucleus with an electric quadrupole moment that can interact with electric field gradients. The anisotropic interaction gives rise to a broad NMR spectrum spanning 100–200 kHz for stationary samples. The ^{2}H NMR line shape is strongly sensitive to the dynamics of the molecule (Eastman et al., 2011; Rice et al., 1981; Spiess, 1983; Vold, 1994). Thus, the line width of the ^{2}H NMR spectrum can be an indicator of the pore size and binding affinity. The static ^{2}H NMR spectra were acquired for the deuterated phenanthrene adsorbed on activated biochar. The broad NMR spectra spanning ∼200 kHz are a characteristic static ^{2}H NMR spectrum from rigid molecules, which were observed in the spectra from N-500AC and N-700AC, suggesting that phenanthrene is tightly bound to these activated biochars. On the other hand, the deuterated sorbate on N-300AC exhibits much narrower line-shape with stronger signal centered at 0 Hz. The narrow ^{2}H NMR spectrum clearly indicates that the sorbate molecule undergoes more significant motions on the surface of N-300AC. The less tightly bound phenanthrene on the N-300AC appears contradictory to the higher sorption efficiency of the N-300AC biochar, since the more dynamic sorbate molecule suggests weaker interactions between the sorbate and biochar.

The tighter binding on the N-500AC may be just because of the restricted motions of the sorbate molecules trapped in smaller pores with limited surface area. However, the ^{2}H NMR spectra were collected after 3 min adsorption where small amount of sorbate (26 mg g^{-1}) is adsorbed on the activated biochar. In addition, the ^{2}H NMR spectrum measured from the fully saturated sample was identical to those from the sample incubated for 3 min. These results indicate that the tight binding on the N-500AC arises from the stronger interaction between the biochar and the sorbate rather than from more limited space available for the sorbate. Our quantitative structural analyses showed that N-500AC has a higher aromaticity and a larger aromatic cluster based on the non-protonated carbon fraction than N-300AC (Table 2), suggesting that the hydrophobic phenanthrene is more tightly bound to N-500AC with stronger π–π interactions. Thus, the better sorption capacity and the higher initial adsorption rate of N-300AC particularly at the short incubation time may arise not only from its larger surface area and pore volume (mesopore), which may

accommodate more sorbate molecules, but also from the smaller entropy change. The binding of the free molecule to the surface is highly unfavorable in terms of entropy, and adsorption on the larger surface area (pore) may minimize the loss of entropy, compensating for the weaker interactions (enthalpy–entropy compensation). In addition, the larger pores in N-300AC may be more readily accessible to the contaminants than those in other activated carbons tested in this study. The tighter binding of the sorbate molecule on N-500AC and N-700AC may also lead to the slow diffusion of sorbates and subsequently less adsorption efficiency of the activated biochars.

4. Conclusions

The NMR analysis and surface characterization exhibited more substantial changes in carbon structure and surface properties of the activated biochars, when they were pretreated at lower pyrolysis temperature. The results imply that the condensed carbon structure in severely-treated biochars might be not suitable to make activated carbons with larger surface area and pore volume. The activated carbon from N-300 biochar presented the faster initial sorption rate and the higher equilibrium concentration for phenanthrene adsorption, but the activated N-700 biochar exhibited stronger binding with the sorbate. These observations suggest the possibilities of designing appropriate adsorbents for specialized application needs.

References

Azargohar, R., Dalai, A.K., 2008. Steam and KOH activation of biochar: experimental and modeling studies. Micropor. Mesopor. Mater. 110, 413–421.

Boving, T.B., Zhang, W., 2004. Removal of aqueous-phase polynuclear aromatic hydrocarbons using aspen wood fibers. Chemosphere 54, 831–839.

Brewer, C.E., Schmidt-Rohr, K., Satrio, J.A., Brown, R.C., 2009. Characterization of biochar from fast pyrolysis and gasification systems. Environ. Prog. Sustain. 28, 386–396.

Brewer, C.E., Unger, R., Schmidt-Rohr, K., Brown, R.C., 2011. Criteria to select biochars for field studies based on biochar chemical properties. Bioenergy Res., 1–12.

Chan, K.Y., Van Zwieten, L., Meszaros, I., Downie, A., Joseph, S., 2007. Agronomic values of green waste biochar as a soil amendment. Aust. J. Soil Res. 45, 629–634.

Chen, B., Chen, Z., 2009. Sorption of naphthalene and 1-naphthol by biochars of orange peels with different pyrolytic temperatures. Chemosphere 76, 127–133.

Chun, Y., Sheng, G., Chiou, C.T., Xing, B., 2004. Compositions and sorptive properties of crop residue-derived chars. Environ. Sci. Technol. 38, 4649–4655.

Czimczik, C.I., Preston, C.M., Schmidt, M.W.I., Werner, R.A., Schulze, E.D., 2002. Effects of charring on mass, organic carbon, and stable carbon isotope composition of wood. Org. Geochem. 33, 1207–1223.

Eastman, M.A., Brothers, L.A., Nanny, M.A., 2011. ^{2}H NMR study of dynamics of benzene-d(6) interacting with humic and fulvic acids. J. Phys. Chem. A 115, 4359–4372.

Figueiredo, J.L., Pereira, M.F.R., Freitas, M.M.A., Orfao, J.J.M., 1999. Modification of the surface chemistry of activated carbons. Carbon 37, 1379–1389.

Global Activated Carbon Market Forcast and Opportunities, 2012. <www.reportlinker.com/p0937503/Global-Activated-Carbon-Market-Forecast-and-Opportunities.html>.

Ho, Y.S., McKay, G., 1998. Sorption of dye from aqueous solution by peat. Chem. Eng. J. 70, 115–124.

Holtman, K.M., Chang, H.M., Jameel, H., Kadla, J.F., 2006. Quantitative C-13 NMR characterization of milled wood lignins isolated by different milling techniques. J. Wood Chem. Technol. 26, 21–34.

Hu, Z., Srinivasan, M.P., 1999. Preparation of high-surface-area activated carbons from coconut shell. Micropor. Mesopor. Mater. 27, 11–18.

Huang, Y., Zhang, J., Zhu, L., 2013. Evaluation of the application potential of bentonites in phenanthrene bioremediation by characterizing the biofilm community. Bioresour. Technol. 134, 17–23.

Kong, H., He, J., Gao, Y., Wu, H., Zhu, X., 2011. Cosorption of phenanthrene and mercury(II) from aqueous solution by soybean stalk-based biochar. J. Agric. Food Chem. 59, 12116–12123.

Larsen, F.H., Jakobsen, H.J., Ellis, P.D., Nielsen, N.C., 1998. QCPMG-MAS NMR of half-integer quadrupolar nuclei. J. Magn. Reson. 131, 144–147.

Li, W., Peng, J., Zhang, L., Yang, K., Xia, H., Zhang, S., Guo, S.H., 2009. Preparation of activated carbon from coconut shell chars in pilot-scale microwave heating equipment at 60 kW. Waste Manage. 29, 756–760 (Oxford).

Lima, I.M., Boateng, A.A., Klasson, K.T., 2010. Physicochemical and adsorptive properties of fast-pyrolysis bio-chars and their steam activated counterparts. J. Chem. Technol. Biotechnol. 85, 1515–1521.

Mao, J.D., Schmidt-Rohr, K., 2003. Recoupled long-range C–H dipolar dephasing in solid-state NMR, and its use for spectral selection of fused aromatic rings. J. Magn. Reson. 162, 217–227.

Moreno-Castilla, C., 2004. Adsorption of organic molecules from aqueous solutions on carbon materials. Carbon 42, 83–94.

Novak, J.M., Busscher, W.J., Laird, D.L., Ahmedna, M., Watts, D.W., Niandou, M.A.S., 2009. Impact of biochar amendment on fertility of a southeastern coastal plain soil. Soil Sci. 174, 105–112.

Park, J., Meng, J., Lim, K.H., Rojas, O.J., Park, S., 2013. Transformation of lignocellulosic biomass during torrefaction. J. Anal. Appl. Pyrol. 100, 199–206.

Peng, R.H., Xiong, A.S., Xue, Y., Fu, X.Y., Gao, F., Zhao, W., Tian, Y.S., Yao, Q.H., 2008. Microbial biodegradation of polyaromatic hydrocarbons. FEMS Microbiol. Rev. 32, 927–955.

Rice, D.M., Wittebort, R.J., Griffin, R.G., Meirovitch, E., Stimson, E.R., Meinwald, Y.C., Freed, J.H., Scheraga, H.A., 1981. Rotational jumps of the tyrosine side-chain in crystalline enkephalin – H-2 NMR line-shapes for aromatic ring motion in solids. J. Am. Chem. Soc. 103, 7707–7710.

Sarkar, B., Xi, Y.F., Megharaj, M., Krishnamurti, G.S.R., Bowman, M., Rose, H., Naidu, R., 2012. Bioreactive organoclay: a new technology for environmental remediation. Crit. Rev. Environ. Sci. Technol. 42, 435–488.

Solum, M.S., Pugmire, R.J., Grant, D.M., 1989. C-13 solid-state NMR of argonne premium coals. Energy Fuel 3, 187–193.

Spiess, H.W., 1983. Molecular-dynamics of solid polymers as revealed by deuteron NMR. Colloid. Polym. Sci. 261, 193–209.

Sun, K., Ro, K., Guo, M., Novak, J., Mashayekhi, H., Xing, B., 2011. Sorption of bisphenol A, 17alpha-ethinyl estradiol and phenanthrene on thermally and hydrothermally produced biochars. Bioresour. Technol. 102, 5757–5763.

Uchimiya, M., Klasson, K.T., Wartelle, L.H., Lima, I.M., 2011. Influence of soil properties on heavy metal sequestration by biochar amendment: 1. Copper sorption isotherms and the release of cations. Chemosphere 82, 1431–1437.

Valderrama, C., Gamisans, X., de las Heras, X., Farran, A., Cortina, J.L., 2008. Sorption kinetics of polycyclic aromatic hydrocarbons removal using granular activated carbon: intraparticle diffusion coefficients. J. Hazard. Mater. 157, 386–396.

Voice, T.C., Pak, D., Zhao, X., Shi, J., Hickey, R.F., 1992. Biological activated carbon in fluidized bed reactors for the treatment of groundwater contaminated with volatile aromatic hydrocarbons. Water Res. 26, 1389–1401.

Vold, R.R., 1994. Nuclear Magnetic Resonance Probes of Molecular Dynamics. Kluwer Academic Publishers, Norwell, MA.

Woolf, D., Amonette, J.E., Street-Perrott, F.A., Lehmann, J., Joseph, S., 2010. Sustainable biochar to mitigate global climate change. Nat. Commun. 1.

Yang, H.P., Yan, R., Chen, H.P., Lee, D.H., Zheng, C.G., 2007. Characteristics of hemicellulose, cellulose and lignin pyrolysis. Fuel 86, 1781–1788.